Cell Stem Cell
Article

Proliferation-Dependent Alterations of the DNA Methylation Landscape Underlie Hematopoietic Stem Cell Aging

Isabel Beerman,[1,2,3] Christoph Bock,[3,4] Brian S. Garrison,[1,2,3] Zachary D. Smith,[3,4] Hongcang Gu,[4] Alexander Meissner,[3,4,5,*] and Derrick J. Rossi[1,2,3,5,*]
[1]Program in Cellular and Molecular Medicine, Division of Hematology/Oncology, Boston Children's Hospital, Boston, MA 02116, USA
[2]Department of Pediatrics, Harvard Medical School, Boston, MA 02115, USA
[3]Department of Stem Cell and Regenerative Biology, Harvard University, Cambridge, MA 02138, USA
[4]Broad Institute of MIT and Harvard, Cambridge, MA 02142, USA
[5]Harvard Stem Cell Institute, Cambridge, MA 02138, USA
*Correspondence: alexander_meissner@harvard.edu (A.M.), derrick.rossi@childrens.harvard.edu (D.J.R.)
http://dx.doi.org/10.1016/j.stem.2013.01.017

SUMMARY

The functional potential of hematopoietic stem cells (HSCs) declines during aging, and in doing so, significantly contributes to hematopoietic pathophysiology in the elderly. To explore the relationship between age-associated HSC decline and the epigenome, we examined global DNA methylation of HSCs during ontogeny in combination with functional analysis. Although the DNA methylome is generally stable during aging, site-specific alterations of DNA methylation occur at genomic regions associated with hematopoietic lineage potential and selectively target genes expressed in downstream progenitor and effector cells. We found that age-associated HSC decline, replicative limits, and DNA methylation are largely dependent on the proliferative history of HSCs, yet appear to be telomere-length independent. Physiological aging and experimentally enforced proliferation of HSCs both led to DNA hypermethylation of genes regulated by Polycomb Repressive Complex 2. Our results provide evidence that epigenomic alterations of the DNA methylation landscape contribute to the functional decline of HSCs during aging.

INTRODUCTION

Adult tissue-specific stem cells function to mediate homeostasis and regenerative potential of organs and tissues. Because these processes deteriorate with advanced age, stem cell decline has been proposed to be a major factor underlying aging-associated degenerative and pathological attributes in various tissues (Rossi et al., 2008; Van Zant and Liang, 2003). In the hematopoietic system, advanced age is accompanied by onset of a number of clinically significant conditions, including diminished competence of the adaptive immune system, reduced regenerative potential, and markedly elevated incidences of myelogenous diseases, including myelodysplastic syndromes and leukemias (Beerman et al., 2010b). Aging of the hematopoietic stem cell (HSC) compartment is believed to centrally contribute to the onset of these pathologies (Rossi et al., 2008; Van Zant and Liang, 2003). The molecular basis for HSC aging is complex, and multiple mechanistic drivers have been identified. These include the following: deregulation of the molecular control of lineage specification (Rossi et al., 2005), activation of inflammatory signaling cascades (Chambers et al., 2007), loss of cell polarity (Florian et al., 2012), dominance of lineage-biased HSC clones (Beerman et al., 2010a; Challen et al., 2010; Dykstra et al., 2011; Muller-Sieburg et al., 2004), and DNA damage accumulation (Rossi et al., 2007; Rübe et al., 2011; Wang et al., 2012; Yahata et al., 2011). It is clear, however, that these mechanisms do not account for all of the cellular and molecular attributes accompanying HSC aging, indicating that other mechanisms must be involved.

Numerous studies have suggested a critical role for epigenetic regulation of HSC central properties, including self-renewal and multilineage differentiation (Oh and Humphries, 2012). Because these stem cell properties are characteristically altered during HSC aging (Rossi et al., 2008), this raises the possibility that age-associated changes in the epigenomic landscape or in its regulators may play a mechanistic role in HSC decline during aging. This is supported by studies demonstrating age-associated deregulation of transcription at distinct chromosomal regions (Chambers et al., 2007) and of gene sets involved in myeloid and lymphoid lineage commitment in HSCs purified from old mice and humans (Chambers et al., 2007; Pang et al., 2011; Rossi et al., 2005), which suggests a mechanism involving coordinated genome-wide regulatory control. That age-dependent epigenomic alterations may be involved in mediating such changes is supported by evidence showing that genes involved in mediating higher-order chromatin structure, chromatin remodeling, and epigenetic regulation are deregulated in HSCs during aging (Chambers et al., 2007; Rossi et al., 2005).

Here, we have investigated the role alterations of the epigenomic landscape play during HSC aging by examining global DNA methylation in these rare stem cells during ontogeny. We show that DNA methylation changes during HSC aging occur at regions associated with lineage potential and principally target genes expressed downstream of HSCs. We also demonstrate

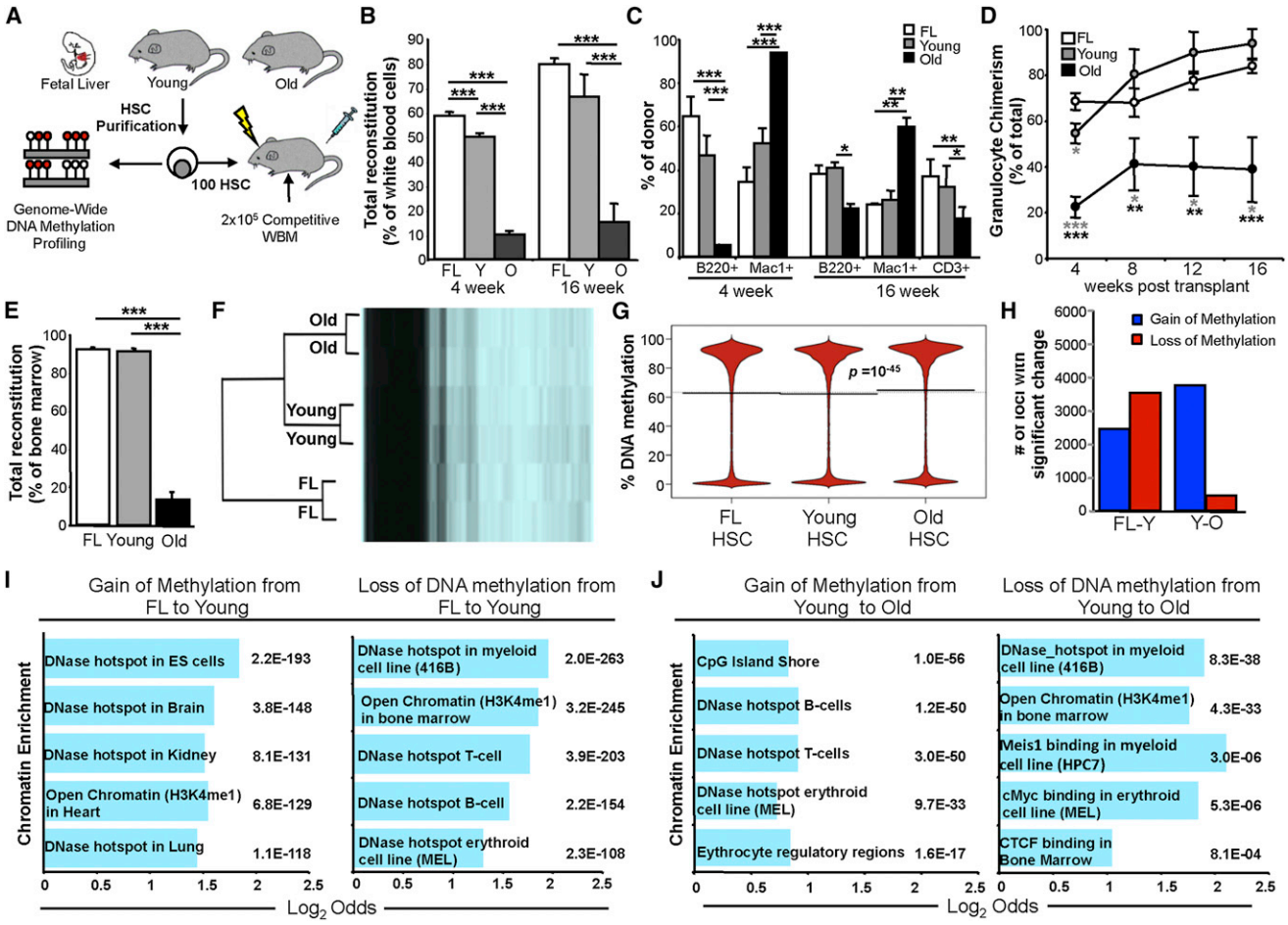

Figure 1. The Functional Potential of HSCs during Ontogeny Is Accompanied by Locus Specificity in the DNA Methylation Landscape

(A) Schematic overview of experimental design.

(B–D) Competitive transplantation of 100 HSCs from fetal liver (FL), young donors (Y), and old donors (O) (n = 8 recipients each) showing (B) total reconstitution, (C) contribution to B cells (B220+) and myeloid (Mac1+) and T cells (CD3+), and (D) granulocyte chimerism at indicated time points.

(E) Bone marrow reconstitution 20 weeks posttransplant of recipients described in (B)–(D).

(F) Hierarchical clustering of representative 1 kb tiles of DNA methylation data of FL-HSCs, young HSCs, and old HSCs.

(G) Bean plots of global DNA methylation of FL-HSCs, young HSCs, and old HSCs.

(H) Number of 1 kb tiles with significant methylation differences in pairwise comparisons between HSCs isolated from different stages of ontogeny. Total comparisons with sufficient DNA methylation data from both populations: FL-Y = 98,112, Y-O = 98,635.

(I and J) Chromatin enrichment of regions with significant methylation changes from FL-HSCs to young HCs (I) and young to old HSCs (J) showing Q values and Log_2Odds scores.

Significant differences: *p < 0.05, **p < 0.01, ***p < 0.001 (t test). Error bars show SEM. See also Figures S1 and S2, Table S1, Table S2, Table S3, and Table S4.

that HSC functional potential, total replicative potential, and differential DNA methylation are dependent on the divisional history of HSCs and concomitant with selective hypermethylation of loci that are normally regulated by Polycomb Repressive Complex 2 (PRC2). Our results are consistent with a central mechanistic role for age-associated epigenetic alterations in mediating the functional decline of HSCs during aging.

RESULTS

The Functional Potential of HSCs during Ontogeny Is Accompanied by Specific DNA Methylation Alterations

To explore the possibility that epigenomic alterations play a role in mediating age-associated HSC functional decline, we purified HSCs from different stages of ontogeny from fetal development through to old age using stringent cell surface criteria (Figure S1A available online) and, in parallel, subjected them to functional assays and genome-wide DNA methylation analysis (Figure 1A). To address functional potential, 100 HSCs from E14.5 fetal liver (FL) and adult bone marrow (BM) of young (3.5-month-old) and old (25-month-old) mice were competitively transplanted into lethally irradiated congenic recipients. Peripheral blood analysis at monthly intervals showed that while FL-HSCs had a slight but significant short-term repopulation advantage over HSCs from young mice, by 16 weeks posttransplant the HSCs from these two stages of ontogeny were comparable in terms of their total repopulating potential (Figures 1B and S1B) and in their ability to give rise to lymphoid and myeloid

effector cells (Figures 1C and 1D). In contrast, HSCs from old mice had impaired total reconstituting potential both short-term (4 weeks) and long-term (16 weeks) posttransplant (Figures 1B and S1B). Consistent with previous reports comparing young and old HSCs (Rossi et al., 2005; Sudo et al., 2000), the lineage potential of HSCs from old mice was skewed toward myeloid reconstitution, whereas FL-HSCs and young HSCs showed balanced reconstitution (Figure 1C). Granulocyte chimerism analysis, which can be used as a surrogate to measure ongoing HSC potential (Bryder et al., 2006), revealed that whereas FL-HSCs and young HSCs showed comparable activity throughout the transplantation time course, aged HSCs showed markedly diminished activity at all time points, consistent with a significant loss of functional potential (Figures 1D and S1B). BM analysis of recipient mice 5 months posttransplant showed that whereas FL-HSCs and young HSCs were again functionally comparable, both far exceeded the old HSCs in their ability to reconstitute the BM (Figure 1E). In contrast, reconstitution of the primitive stem/progenitor compartment, including phenotypic HSCs and Flk2$^-$ multipotent progenitors (MPP^{Flk2-}, sometimes referred to as ST-HSCs), was comparable regardless of donor age (Figure S1C) consistent with previous reports demonstrating the sustained potential of old HSCs to reconstitute the primitive stem cell compartment (Rossi et al., 2005). However, in line with their diminished lymphoid lineage potential (Figure 1C), old HSCs poorly reconstituted the more committed Flk2$^+$ multipotent progenitors (MPP^{Flk2+}), which include the lymphoid-primed multipotent progenitor (LMPP) subpopulation (Adolfsson et al., 2005) (Figure S1C).

Genome-wide DNA methylation analysis using reduced representation bisulfite sequencing (RRBS) was performed in parallel on the HSCs purified from FL and adult young and old BM, which provided single-CpG-resolution data from these rare populations (Gu et al., 2011; Smith et al., 2012). DNA methylation measurements were obtained from, at minimum, two biological replicates (Table S1). Resulting data sets covered most CpG islands and annotated gene promoters and provided a representative sampling of putative enhancers and CpG island shores. Consistent with the established reproducibility of the technology (Bock et al., 2010; Meissner et al., 2008), we observed excellent correlation (Pearson's $r > 0.98$) between all biological replicates when the data was analyzed either at the nucleotide level or as 1 kb genomic tiles (Figure S2A and Table S2). Strikingly, pairwise comparisons between FL-HSCs, young HSCs, and old HSCs were highly correlated (Pearson's $r > 0.97$), indicating that the DNA methylation landscape is largely stably maintained during HSC ontogeny (Figure S2B and Table S2). Despite this overall similarity, however, hierarchical clustering analysis of the methylation profiles showed that HSCs from defined stages of ontogeny clustered independently, which indicated unique age-associated methylation signatures (Figure 1F). Interestingly, a slight but significant increase in global methylation was evident in the HSCs isolated from old mice (Figure 1G), an observation that stands in marked contrast to the results of a number of studies reporting global DNA hypomethylation in aged somatic cells and tissues from diverse species (Gonzalo, 2010).

To define the differences contributing to the unique age-associated DNA methylation signatures, we conducted pairwise comparisons that led to the identification of several thousand loci that significantly gained or lost DNA methylation during HSC ontogeny (Figures 1H and S2C and Table S3 and Table S4). These methylation differences mapped throughout the genome and showed limited enrichment to specific chromosomal regions (Figure S2D), though they tended to cluster at regions with high guanine-cytosine (GC) content, as expected (Figure S2E). To address how these changes in DNA methylation might impact the function of HSCs during ontogeny, we analyzed the differentially methylated DNA regions identified during HSC ontogeny in comparison to genomic features functionally annotated by ENCODE (Thomas et al., 2007) and defined in other publicly available data sets, as we previously described (Bock et al., 2012). Genomic regions that gained methylation in the transition from FL-HSCs to young HSCs were significantly enriched for regions of open chromatin in nonhematopoietic cells, including DNase hotspots in embryonic stem cells, brain, kidney, and lung, in nonhematopoietic cells, whereas regions that lost DNA methylation during this transition were enriched for regions of open chromatin in blood cells (Figure 1I). Nonetheless, the observed methylation differences between FL-HSCs and young HSCs do not appear to significantly influence hematopoietic potency because HSCs from FL and young mice exhibited near equal potential in the transplantation assays we performed (Figures 1B–1E). In contrast, the DNA methylation differences between young and old HSCs localized to genomic regions that more readily reflected the differences observed in lineage potential of aged HSCs both at steady state (Figure S1D) and after transplantation (Figure 1C). For example, increased DNA methylation during this transition was enriched at regions of open chromatin in erythroid, B, and T cells, whereas loss of methylation was enriched at regions of open chromatin in myeloid cells (Figure 1J). These observations are consistent with the idea that locus-specific DNA methylation alterations, by restricting access to chromatin regions associated with these lineages, contribute to the diminished lymphoid and erythrocyte potential of old HSCs (Figures 1C and S1D). In contrast, no obvious link between differential DNA methylation and the diminished total reconstituting potential of HSCs from old mice was evident. This suggests that this latter aspect of HSC aging may be more strictly under the control of different mechanistic drivers, such as DNA damage accrual (Mandal et al., 2011).

DNA Methylation Changes during HSC Ontogeny Largely Target Genes Expressed in Downstream Hematopoietic Progeny

To examine the relationship between ontogeny-associated HSC DNA methylation changes and gene expression, we performed genome-wide expression profiling on HSCs purified from FL and young and old mice. Hierarchical clustering analysis of the resulting expression profiles revealed that HSCs from these defined stages of ontogeny clustered separately (Figure 2A), and similar to the methylation profiles (Figure 1F), HSCs from young and old mice clustered more tightly to each other than to FL-HSCs. This analysis revealed complex age-associated expression patterns of genes, including *Dnmt1*, *Dnmt3a* and *Dnmt3b*, *Tet1*, *Tet2*, and *Uhrf1*, involved in mediating DNA methylation dynamics (Figure S3A). Differentially expressed genes were then globally defined (fold change $\geq$ 2.0, $p \leq 0.001$,

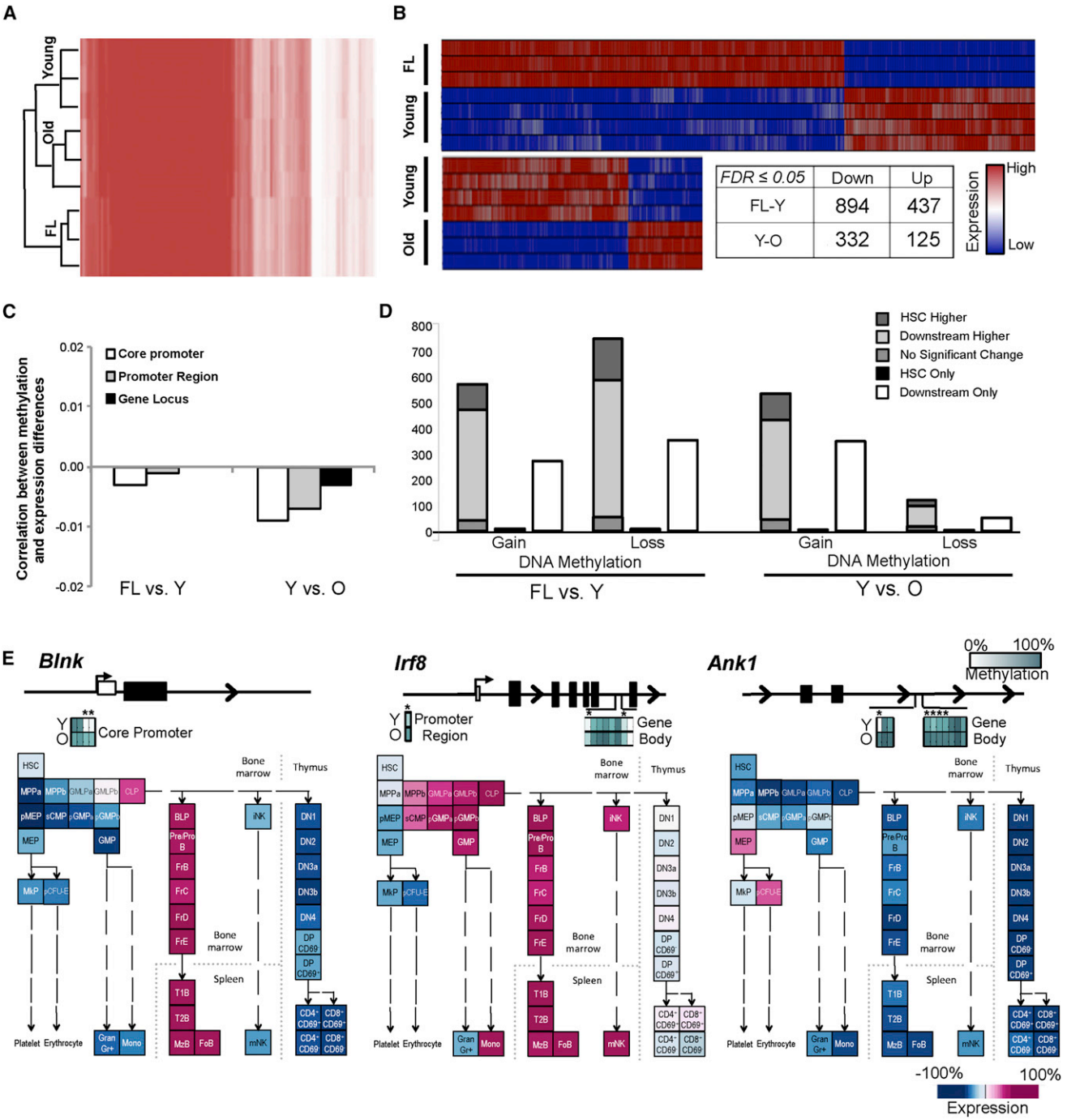

Figure 2. DNA Methylation Changes during HSC Ontogeny Largely Target Genes Expressed in Downstream Hematopoietic Progeny

(A) Hierarchical clustering of representative expression profiles of FL-HSCs, young HSCs, and old HSCs.

(B) Heatmap plots of relative gene expression profiles with ≥2× expression change, $p \leq 0.001$, and FDR ≤ 0.05 between ontogeny stages.

(C) Correlation between differences in DNA methylation of core promoters, promoter regions, and gene loci with expression.

(D) Genes showing significant changes in DNA methylation expressed in ≥1 of 39 hematopoietic cell types during transitions of ontogeny. Genes expressed in HSCs and downstream cells (leftmost of each comparison group) were categorized as significantly higher in HSCs compared to downstream cells (HSC higher), significantly higher in downstream cells compared to HSCs (Downstream higher), and having no significant changes in expression. Significant expression differences were defined as ≥1.5-fold average expression with $p \leq 0.01$. Remaining genes were exclusively expressed in HSCs (HSC only, middle of each comparison group), or exclusively expressed in downstream progeny (Downstream only, rightmost of each comparison group).

(E) Representative genes with significant DNA methylation differences in old compared to young HSCs expressed exclusively in downstream cells. DNA methylation differences and gene expression pattern in hematopoiesis are shown (Seita et al., 2012). Gene regions presented are *Blnk*,

(legend continued on next page)

FDR $\leq$ 5%), and by these criteria, 1331 and 457 genes were identified as differentially expressed in the transitions from FL-HSCs to young HSCs, and young to old HSCs, respectively (Figure 2B and Table S5). We next correlated differences in gene expression to DNA methylation and found no correlation in the genes differentially expressed during the FL-HSC to young HSC transition, and we found only a modest negative correlation, which was most pronounced at core promoter and promoter regions, in the transition from young to old HSCs (Figures 2C and S3B). These results are consistent with previous studies demonstrating little global correlation between gene expression and DNA methylation in diverse cell types (Bock et al., 2012; Challen et al., 2012; Deaton and Bird, 2011).

Our functional data, combined with our observation that DNA methylation at chromatin regions associated with downstream lineages was altered during HSC aging (Figure 1), raised the possibility that the differential methylation observed during HSC ontogeny may target genes expressed in downstream progeny of HSCs. We therefore sought to explore the relationship between the DNA methylation changes observed during HSC ontogeny and gene expression throughout hematopoiesis. Toward this we used microarray data, generated by others and ourselves, of 39 different FACS-purified hematopoietic cell types comprising the vast majority of hematopoietic stem, progenitor, and effector cells (Seita et al., 2012) (Figure S3C). We mapped the significant gains and losses of DNA methylation during HSC ontogeny to gene loci and then correlated these DNA methylation changes to gene expression in each of the 39 hematopoietic subsets. This analysis revealed that the largest numbers of genes showing significant gains or losses of DNA methylation were expressed in HSCs and their downstream progeny (Figure 2D and Table S6). Of these, it was nonetheless striking that in all cases, the vast majority of these genes were more highly expressed in downstream hematopoietic progenitors and effectors than in HSCs themselves ($\geq$1.5-fold, $p \leq 0.01$, Figure 2D). Interestingly, only very few genes differentially DNA methylated during HSC ontogeny were exclusively expressed in HSCs (Figure 2D). In striking contrast, a large number of DNA methylated genes were exclusively expressed in downstream progenitor and effector cells, but not in HSCs themselves (Figure 2D). Among this latter class were genes important for the development, specification, and function of diverse hematopoietic cell types, including lymphoid and erythroid lineages, both of which are diminished upon hematopoietic aging in mouse and man (Figures 1C and S1D) (Beerman et al., 2010b; Ewing and Tauber, 1964). For example, old HSCs showed significant gains of DNA methylation at the core promoter of *Blnk*, a signal adaptor molecule that is required for B cell development (Pappu et al., 1999) and only expressed downstream of HSCs in the B cell lineage starting at the CLP stage (Figure 2E). Another interesting gene expressed downstream of HSCs that gained methylation in old HSCs, this time within the promoter region and gene body, was *Irf8* (Figure 2E), which encodes a transcription factor that upon conditional deletion leads to impaired B cell development and concomitant skewing to myeloid fates (Wang et al., 2008). In contrast, *Ank1*, which is strictly expressed in erythroid progenitors and plays a critical role in erythroid development (Rank et al., 2009), showed DNA hypermethylation only within the gene body in old HSCs (Figure 2E).

Taken together, these results indicate that the DNA methylation dynamics underlying HSC ontogeny only modestly correlate with gene expression in HSCs and instead largely target genes exclusively or more highly expressed in downstream progenitor and effector cells. This suggests that age-associated DNA methylation changes in HSCs may predominantly influence the transcriptional competence of genes that become activated during HSC differentiation to defined lineages.

Induced HSC Proliferation Leads to Functional Decline and DNA Methylation Changes that Closely Mimic Physiological HSC Aging

In adults, HSCs are predominantly quiescent and cycle infrequently. Estimates suggest that adult HSCs undergo 5–20 divisions over the course of a 2 year life span (Foudi et al., 2008; Wilson et al., 2008). To investigate the impact of cell division on HSC function and DNA methylation, we treated young adult mice with 5-Fluorouracil (5-FU), which selectively kills cycling cells leading to HSC proliferation. To selectively drive HSCs to different degrees of proliferation, mice received zero, two (2×), or four (4×) administrations of 150 mg/kg of 5-FU at 3 week intervals, and 2 months after the final injection, HSCs were subjected to functional and DNA methylation analysis (Figure 3A). BM analysis of 5-FU-treated mice showed that the treated mice (2× and 4× 5-FU) displayed an increased frequency of LSK cells (Figure 3B), with an increased percentage of HSCs and a decreased percentage of MPP^{Flk2+} (Figure 3C). Interestingly, these changes model the changes in the primitive stem and progenitor compartment of naturally aged mice (Figure 3C) (Beerman et al., 2010a; de Haan et al., 1997; Rossi et al., 2005). However, unlike in normal physiological HSC aging (Beerman et al., 2010a), costaining HSCs with CD150, which we and others have previously shown can be used to subfractionate functionally distinct HSCs subsets (Beerman et al., 2010a; Morita et al., 2010), showed comparable HSC subset composition between the untreated and 5-FU treated cohorts, indicating that 5-FU treatment did not lead to experimental selection of HSC subtypes (Figure 3D).

BM cells from treated and untreated mice were competitively transplanted, which showed that the HSCs subjected to the greatest proliferative challenge (4× 5-FU) were impaired in their total reconstitution potential in both the short term and long term posttransplant (Figure 3E). These heavily challenged HSCs also exhibited a skewing of their lineage potential (Figure 3F) that closely mimicked physiologic HSC aging (Figure 1C). Granulocyte chimerism, measured throughout the course of the experiment, and BM reconstitution measured at 20 weeks posttransplant revealed trends of diminished HSC functional

chr19: 41,060,000–41,072,000; *Irf8*, chr8: 123,248,000–123,277,000; and *Ank1*, chr8: 24,251,000–24,257,000. Single CpGs with significant differential DNA methylation are denoted with asterisks (*). Transcription start sites (TSS, tall arrow), untranscribed regions (white boxes) and exons (black boxes) are shown. Promoter Region: −20 kb of TSS; Core Promoter: −5 kb to +1 kb of TSS; Gene Body: within gene.
See also Figure S3, Table S5, and Table S6.

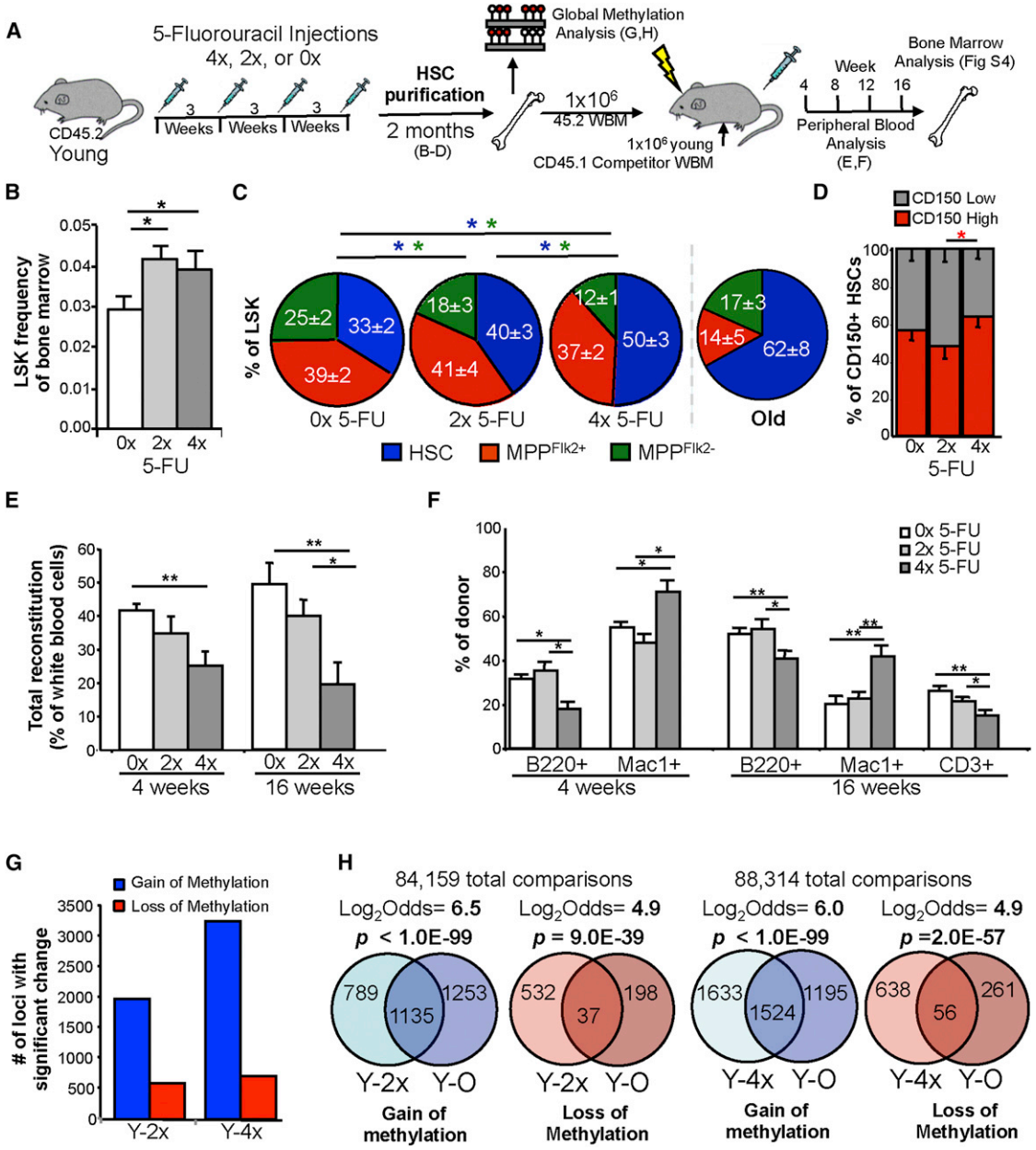

Figure 3. Increased HSC Proliferation Leads to Functional Decline and Differential DNA Methylation that Recapitulates Physiological HSC Aging

(A) Schematic overview of experimental design.

(B–D) Bone marrow analysis of mice receiving four (4×), two (2×) or zero (0×) administrations of 5-fluorouracil (5-FU) (n = 8) 2 months postfinal 5-FU administration. Shown are (B) the primitive LSK compartment and (C) breakdown of the primitive LSK compartment as follows: HSC ($CD34^-$ $Flk2^-$), MPP^{Flk2-} ($CD34^+$ $Flk2^-$) and MPP^{Flk2+} ($CD34^+$ $Flk2^+$), and LSK compartment of old mice (right), with (D) CD150 subsets of HSCs (Beerman et al., 2010a; Morita et al., 2010).

(E and F) Total reconstitution of recipient mice transplanted with 1 × 10^6 WBM cells from mice that received 4×, 2×, or 0× 5-FU against 1 × 10^6 young competitor BM cells (E) and lineage contribution to B cells (B220+), myeloid cells (Mac1+), and T (CD3+) cells at indicated times posttransplant (F) (n = 6 recipients each).

(G) Number of 1 kb tiles with significant differential DNA methylation as determined by pairwise comparisons between HSCs after 5-FU receipt and HSCs from untreated young (Y) mice. Total comparisons with sufficient DNA methylation information for both populations were as follows: Y-2× = 84,510, Y-4× = 88,704.

(H) Overlap of 1 kb intervals with significant gains or losses of DNA methylation in comparisons between enforced HSC proliferation (2× or 4× 5-FU) either in untreated young HSCs or during HSC aging (young to old) showing p values, Log_2Odds scores, and total comparisons.

Significant differences: *p < 0.05, **p < 0.01, ***p < 0.001 (t test). Error bars show SEM. See also Figure S4.

potential after 5-FU-induced proliferative challenge that were similar to physiologic aging, yet did not reach statistical significance (Figures 1D, 1E, S4A, and S4B).

DNA methylation profiling of HSCs purified from 5-FU-treated and untreated control mice was analyzed in pairwise comparisons as described above, which revealed significant differential

methylation at several thousand loci (Figures 3G and S4C). As we had observed during physiological aging (Figure 1H), regions that gained DNA methylation predominated the observed changes (Figure 3G). This observation, combined with the functional similarity to physiological HSC aging, prompted us to examine whether the sites altered after 5-FU-induced HSC proliferation overlapped with those altered during physiologic HSC aging. Strikingly, a highly significant number of loci that either gained or lost methylation were shared between physiologic HSC aging and young HSCs subjected to the proliferative challenge of repeated 5-FU administration (Figure 3H). Cumulatively, these results indicate that both HSC functional decline and age-associated DNA methylation changes are largely HSC proliferation dependent.

The Replicative Limits of HSCs Are Proliferative History Dependent, Yet Telomere Length Independent

It has previously been shown that HSCs transplanted at lower numbers in primary transplants are subjected to increasingly greater proliferative stress (Pawliuk et al., 1996). We reasoned that if the proliferative history of HSCs played a central role in limiting their functional potential and/or altering their DNA methylation landscape, this would be revealed in such an experimental setting. We therefore purified HSCs from young mice, transplanted limiting numbers of the HSCs over a 50-fold range (500, 50, or 10 cells) into primary recipients, purified them 20 weeks after transplant (Figure S5A), and subjected them to either DNA methylation analysis or serial transplantation (Figures 4A). BM analysis of the primary recipients 20 weeks post-transplant showed that, as expected, the extent of donor reconstitution correlated with number of HSCs originally transplanted (Figure 4B). As in our 5-FU experiments (Figure 3D), examination of the HSC compartment revealed that different HSC subtypes as defined by costaining with CD150 (Beerman et al., 2010a; Morita et al., 2010) were similarly represented regardless of the original HSC numbers transplanted (Figure S5B). Donor-derived HSCs were FACS purified and equal numbers of HSCs (200 cells) were competitively transplanted into secondary recipients (Figure S5A). Peripheral blood analysis of secondary recipients showed an inverse correlation between HSC proliferative history and reconstitution potential—in other words, HSCs that had undergone greater transplant-induced proliferative stress in the primary transplants performed less well, on a per cell basis, in the secondary transplants (Figure 4C). The functional impact of these differences in HSC proliferative history was also reflected throughout the secondary transplants by granulocyte chimerism, which further demonstrated that HSCs from the original 50 and 10 cell transplants became functionally exhausted during the course of secondary reconstitution (Figure 4D). Five months postsecondary transplant, this was confirmed with BM analysis, which showed that only the HSCs that had been subjected to the least amount of proliferative challenge in the primary transplants (500 HSCs) were able to effectively repopulate the BM, whereas those transplanted at the lower doses (50 and 10 HSCs) gave rise to only minimal BM reconstitution in secondary hosts (Figure 4E). These results were largely recapitulated when HSCs from old mice were transplanted at 500, 50, and 10 cell doses and then functionally evaluated by serial transplantation using a similar experimental approach (Figures S5A–S5C). These experiments again demonstrated that only HSCs transplanted at the highest dose (500 HSCs) in the primary transplants were able to give rise to sustained long-term multilineage reconstitution upon secondary transplantation (Figures S5D and S5E).

Although telomere length limits the replication potential of many human cell types, this is generally not believed to be the case in C57BL/6 mice, which are relatively short-lived and have long telomeres. Although progressive telomere attrition has been observed in HSCs during serial transplantation (Allsopp et al., 2001), telomere length does not ultimately appear to limit the replicative capacity of HSCs, which exhaust during serial transplantation even under settings where telomere length is maintained through enforced expression of telomerase (Allsopp et al., 2003). Nonetheless, the proliferation-dependent HSC functional exhaustion observed in our experiments prompted us to examine telomere length. Given the limited donor-derived cell numbers in our transplant experiments, we used a recently developed single-cell qPCR-based strategy to measure relative telomere length (Norddahl et al., 2012) using donor-derived granulocytes as a surrogate for quantifying telomere length in HSCs (Figures S6A–S6D) (Bryder et al., 2006) in both the primary and secondary HSC transplants described above. Strikingly, regardless of original transplant cell number (500, 50, or 10 HSCs), no significant differences were observed in the relative telomere length of donor-derived granulocytes from either the primary or secondary transplants (Figure 4F), despite the fact that the HSCs derived from the mice transplanted at low cell numbers eventually reached their replicative limits and became exhausted (Figure 4D).

Taken together, these results indicate that the total replicative potential of HSCs is ultimately limited by their proliferative history, yet appears to be telomere length independent.

The Replicative Limit of HSCs Is Associated with Global DNA Hypomethylation

DNA methylation analysis of HSCs purified after primary transplantation in these experiments revealed HSCs from young or old donors subjected to increasingly greater transplantation-induced proliferative stress (500 HSCs < 50 HSCs < 10 HSCs) showed significant stepwise global hypomethylation in comparison to steady-state young or old HSCs (Figures 5A and S5F). Consistent with this, pairwise comparisons to steady-state young HSCs showed that regions with significant losses of DNA methylation upon transplant-induced HSC proliferation predominated in all cases (Figures 5B and S5G). These results contrast with our observations of normal physiologic HSC aging (Figures 1G and 1H), and are more in line with the global DNA hypomethylation reported to accompany aging in somatic cells and tissues (Gonzalo, 2010). Nonetheless, comparisons of the loci showing significant differential DNA methylation in these experiments to those observed during steady-state HSC aging revealed a highly significant overlap of specific loci that both gained or lost DNA methylation (gains and losses) (Figures 5C and S5H). These results further support the interpretation that the changes in the DNA methylation landscape observed during HSC aging are, to a great extent, driven by HSC proliferation.

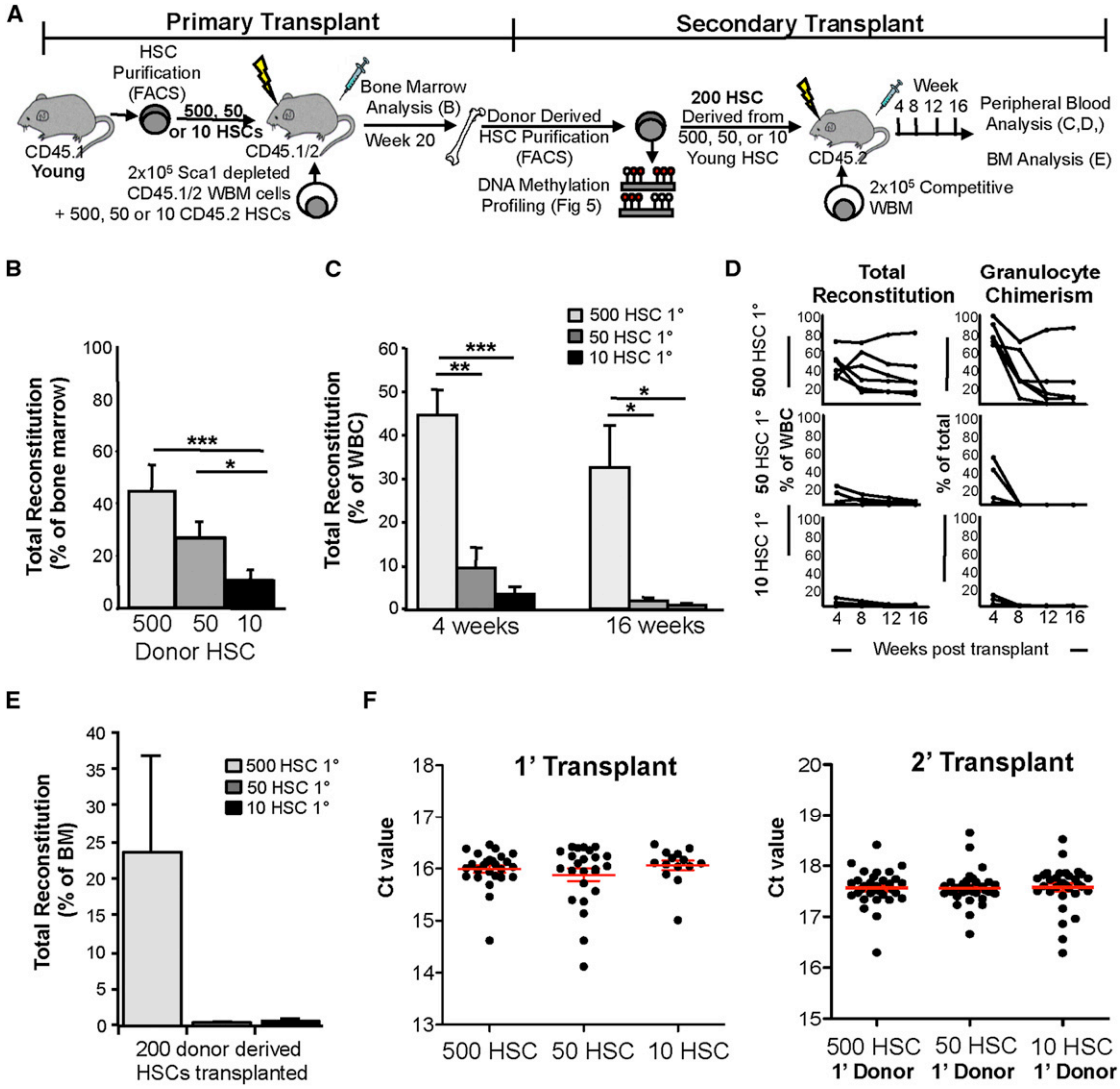

Figure 4. The Replicative Limits of HSCs Are Proliferative History Dependent, Yet Independent of Telomere Length

(A) Schematic overview of experimental design.

(B) Total donor BM reconstitution, 20 weeks posttransplant, of recipient mice transplanted with 500, 50, or 10 young HSCs (CD45.1) and 500, 50, and 10 old HSCs (CD45.2) (respectively) and a radio-protective dose of Sca1-depleted bone marrow cells (CD45.1/2).

(C and D) Competitive secondary transplantation of 200 donor-derived HSCs from the primary transplants of 500, 50, or 10 young HSCs (n = 7, 4, or 5 recipients, respectively) against 2 × 10^5 competitor BM cells showing (C) total reconstitution and (D) granulocyte chimerism.

(E) Total donor BM reconstitution of the recipients described in (B) and (C) 20 weeks postsecondary transplant.

(F) Single-cell qPCR telomere length analysis of donor-derived granulocytes isolated from primary recipients of 500, 50, or 10 young HSCs (left, n≥14) or secondary (right, n≥28) recipients measured at 12 and 8 weeks posttransplant, respectively.

Significant differences: *p < 0.05, **p < 0.01, ***p < 0.001 (t test). Error bars show SEM. See also Figures S5 and S6.

Specific DNA Hypermethylation of PRC2 Target Genes in HSCs after Enforced Proliferation and Aging

To further explore the degree to which proliferative history shapes the epigenetic landscape of HSCs during aging, we performed a meta-analysis comparing the DNA methylation data we generated for normal physiologic HSC aging to all the data sets generated for HSCs subjected to experimentally enforced proliferation (EP). These included data sets of HSCs derived from the 5-FU treated mice (2× and 4× 5-FU) (Figure 3) and HSCs (both young and old) derived from the mice transplanted with 10, 50, or 500 HSCs (Figure 4, Figure 5, and Figure S5). This analysis revealed very significant overlaps of loci that either gained or lost DNA methylation during physiological aging or after EP (Figure 6A), supporting the conclusion that locus-specific changes in the DNA methylome during HSC aging are, to a significant degree, proliferation dependent. Our results demonstrating that HSC functional potential is also largely dependent on the proliferative history of HSCs (Figures 3E and 3F, Figures 4B–4E, and Figures S4A, S4B, S5D, and S5E) prompted us to examine the genes showing aging- and proliferation-dependent

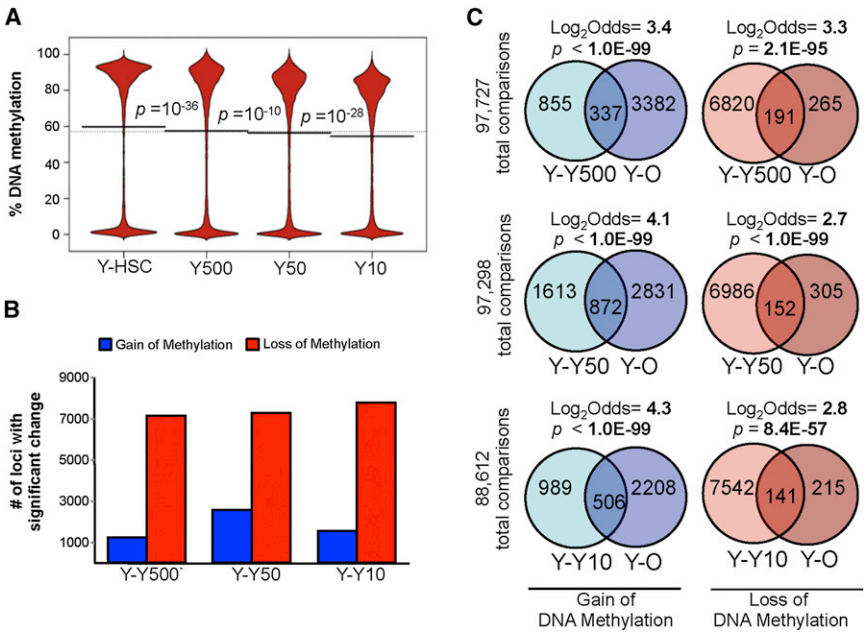

Figure 5. The Replicative Limit of HSCs Is Associated with Global DNA Hypomethylation

(A) Bean plot of global DNA methylation of steady-state young HSCs and donor-derived HSCs isolated from primary recipients of 500, 50, or 10 transplanted young HSCs.

(B) Number of 1 kb tiles with significant DNA methylation differences in pairwise comparisons of HSCs derived from initial transplants of 500, 50, and 10 young HSCs to steady-state young HSCs. Total comparisons with sufficient DNA methylation information for both populations are as follows: Y-Y500 = 98,301, Y-Y50 = 97,872, Y-Y10 = 89,051.

(C) Overlap of 1 kb intervals with significant differential DNA methylation in comparisons between young transplanted HSCs (500, 50, or 10 HSCs) to young HSCs, and also during HSC aging (young to old), showing p values, Log_2Odds scores, and total comparisons.

See also Figure S5.

differential DNA methylation more closely. To this end, we performed gene set enrichment analysis (GSEA) on the genes that consistently gained or lost DNA methylation during HSC aging and after subjection to EP (438 and 97 loci, respectively) (Figure 6A). Whereas no significant enrichments were associated with the genes that lost DNA methylation, the 438 loci that gained DNA methylation were highly enriched with loci marked by H3K27 and bound by EED and SUZ12 in human embryonic stem cells—which together represent the epigenetic mark and two of the core components of Polycomb repressive complex 2 (PRC2) (Figure 6B, Table S7).

Recent studies have shown that chromatin-bound PRC2 and DNA methylation at CpG-dense regions are mutually exclusive (Brinkman et al., 2012; Meissner et al., 2008; Weinhofer et al., 2010). The antagonistic nature of PCR2 and DNA methylation, combined with our results showing that PRC2 targets were selectively DNA hypermethylated upon enforced HSC proliferation and during HSC aging, prompted us to examine the expression of PRC2 core components *Ezh2*, *Suz12*, and *Eed* by qRT-PCR in HSCs purified from young and old mice. We reasoned that diminished levels of PRC2 might facilitate DNA hypermethylation at these specific loci in old HSCs. Consistent with this idea, we found that these PRC2 core components were significantly age downregulated in HSCs, with *Ezh2* showing the greatest fold difference (3.7-fold) and *Suz12* and *Eed* showing more modest downregulation (both 1.4-fold) (Figure 6C).

Taken together, these results demonstrate that PRC2 target genes are selectively DNA hypermethylated in a proliferation-dependent manner during HSC aging, concomitant with age-diminished expression of the PRC2 complex.

DISCUSSION

Numerous lines of evidence have suggested that age-dependent epigenomic alterations may mechanistically contribute to the functional decline of HSCs during aging, yet the paucity of HSCs and technical challenge of profiling the epigenomes of such rare cells has precluded analysis. Herein, we have addressed this issue by using high-throughput bisulfite sequencing to generate DNA methylation profiles of purified HSCs from different stages of ontogeny. To provide functional context to the resulting DNA methylation data, we performed functional experiments on purified HSCs in parallel.

In contrast to FL-HSCs and young adult HSCs, which showed robust activity in transplantation assays with comparable lineage predisposition and reconstituting potential, purified HSCs from old mice showed substantially diminished repopulating activity and a skewing of lineage potential consistent with previous reports (Beerman et al., 2010a; Muller-Sieburg et al., 2004; Rossi et al., 2005; Sudo et al., 2000). Given that the FL is a fundamentally different niche than the BM microenvironment from which both young and old adult HSCs were isolated, these results suggest that chronological aging has greater impact on HSC functional potential than microenvironmental influences. With this said, HSCs of fetal origin do differ from adult HSCs in a number of respects, including immunophenotype, cell cycle status, and ability to give rise to distinct subsets of B cells and T cells (Rossi et al., 2008). It should also be noted that the BM niche of mice changes substantially with advanced age, becoming osteoporotic and infiltrated with adipose tissue. Nonetheless, our results combined with evidence demonstrating the cell-autonomous nature of HSC aging: HSCs from old mice exhibit functional impairment even upon transplantation into young recipients (Rossi et al., 2005), which argues that chronological aging is a major factor underlying HSC functional decline.

Given the aforementioned differences in niche and functional potential of HSCs during ontogeny, it was interesting to see that the DNA methylation landscape of HSCs was very stable from fetal development through to old age, although a slight but significant degree of global DNA hypermethylation was observed in old HSCs. This latter observation contrasts with numerous reports demonstrating that somatic tissues and cells

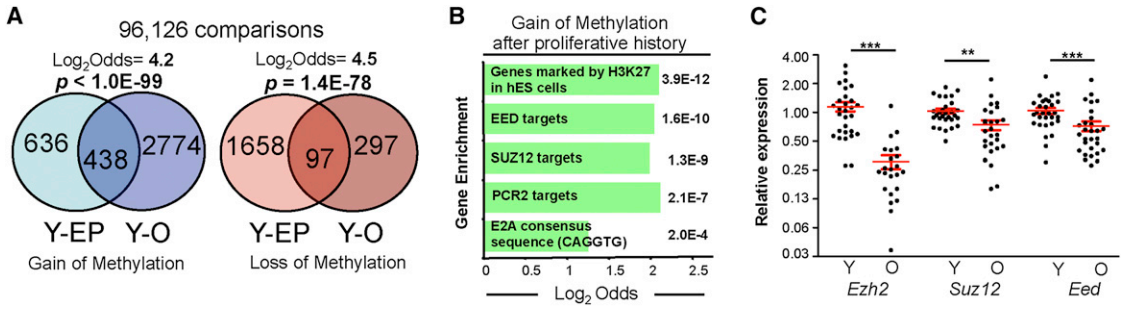

Figure 6. Targeted DNA Hypermethylation of PRC2 Regulated Genes Accompanies Proliferation-Dependent HSC Aging

(A) Overlap of 1 kb intervals with significant differential methylation in composite comparisons of HSCs subjected to experimentally enforced proliferation (EP) to young HSCs (Y) (Y-EP) and during HSC aging (Y-O) showing p values, Log_2Odds scores, and total comparisons. Comparisons include 1 kb regions with methylation information in young and old mice, and at least six of the eight samples subjected to EP with threshold significance set at n-2 with significant changes.

(B) Gene set enrichment analysis of the 438 loci with consistent gains of methylation after EP and during HSC aging identified in (A) showing Q values and Log_2Odds scores.

(C) qPCR-generated relative expression values of PRC2 components from young and old HSCs showing individual measurements of sorted HSCs (10 cells), ($n \geq 23$).

Significant differences: *$p < 0.05$, **$p < 0.01$, ***$p < 0.001$ (t test). Error bars show SEM. See also Table S7.

derived from aged animals frequently present global DNA hypomethylation with advanced age (Gonzalo, 2010). We propose that these differences may reflect the fact that in contrast to somatic cells, which are largely postmitotic, the mitotic potential of HSCs extends far beyond a single life span (Harrison and Astle, 1982). In support of this model, DNA hypomethylation ensued when we experimentally pushed HSCs to their replicative limits by serially transplanting limited numbers of HSCs (Figure 7).

Despite the overall stability of the HSC DNA methylation landscape, minor fractions of the genome were specifically, differentially methylated at different stages of HSC ontogeny. Consistent with the functional comparability of FL and young HSCs, the genomic regions differentially methylated at this transition did not overtly reflect DNA methylation differences that would influence function but rather appeared more suggestive of a process of ongoing developmental restriction: young HSCs gained DNA methylation on regions associated with nonhematopoietic lineages, whereas significant losses of DNA methylation were enriched at genomic regions associated with blood cell production.

In contrast, the transition to old age was marked by gains of DNA methylation at genomic regions associated with open chromatin in lymphoid (B cell and T cell) and erythroid lineages, all of which are diminished during aging (Figures 1C and S1D) (Beerman et al., 2010b). These data suggest that increased methylation at such loci might restrict the potential of old HSCs by inhibiting differentiation toward these lineages, possibly by modulating chromatin accessibility to transcriptional programs active in downstream cells during differentiation. Consistent with this idea, we found that the vast majority of genes differentially methylated during HSC ontogeny were either exclusively expressed downstream of HSCs or expressed at higher levels in progenitor and/or effector cells relative to HSCs. This was an unexpected discovery because it suggests that DNA methylome alterations occurring specifically in HSCs during ontogeny may directly manifest their impact on hematopoietic aging by altering gene programs and transcriptional networks activated during differentiation in downstream progeny, but not in HSCs themselves. With this said, we did not observe overt differences in lineage potential of FL and young HSCs, which were also marked by DNA methylation alterations of genes expressed downstream of HSCs. One potential explanation is that the observed methylation differences in FL-HSCs may influence their properties in a niche-specific manner and have little impact on the potential of these cells after transplantation into adult recipients, which we used to assay their function. It will also be interesting to determine how ontogeny-associated differences in HSC subtypes (Beerman et al., 2010a; Benz et al., 2012; Challen et al., 2010; Dykstra et al., 2007; Morita et al., 2010; Muller-Sieburg et al., 2004; Sudo et al., 2000) contribute to the DNA methylation patterns we observed in this study.

Though the replicative potential of HSCs is extensive, it is exhaustible. Similar to the finite limits of cell doubling (Hayflick and Moorhead, 1961), serial transplantation experiments have demonstrated that HSCs have a finite limit to their replication potential (Harrison and Astle, 1982). However, while telomere attrition is known to limit the replicative capacity of many human cell types, preservation of telomere length through enforced expression of telomerase in murine HSCs does not extend their replicative capacity (Allsopp et al., 2003). This demonstrates that another mechanism must underlie the limits of HSC self-renewal. Using settings of experimentally enforced HSC proliferation, we found that the repopulating potential, lineage potential, and total self-renewal capacity of HSCs is dependent on their divisional history, yet appears to be telomere length independent. Whether a developmentally preordained, fixed number of HSC cell divisions exists, or whether the limits of HSC self-renewal are instead underwritten by mechanisms that could be fostered by cell division, such as DNA damage accumulation, is currently unclear. Nonetheless, the fact that HSC self-renewal is ultimately limited by replicative history may explain why engineered mutations leading to loss of HSC quiescence or sustained cycling frequently lead to premature HSC exhaustion (Rossi et al., 2012).

Unexpectedly, we also found that age-associated alterations of the DNA methylation landscape were dependent, to a large

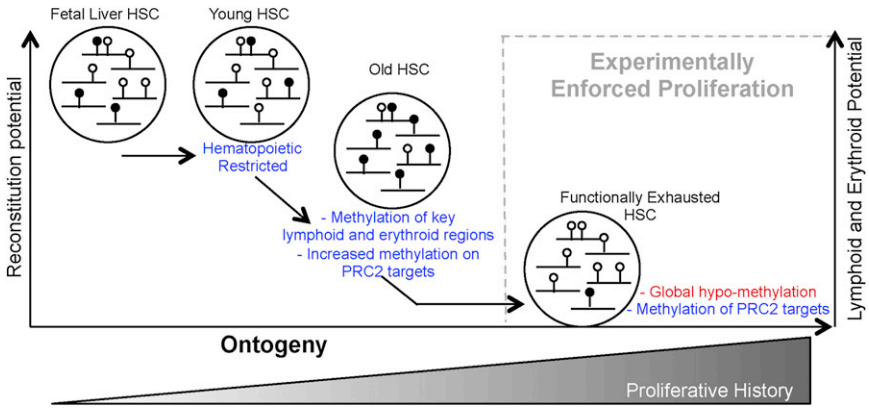

Figure 7. Model of the Changing DNA Methylation Landscape and Functional Potential of HSCs during Ontogeny

Schematic representation of DNA methylation changes in HSCs (white lollipop, unmethylated CpGs; black lollipop, methylated CpGs) and the functional alterations associated with HSC ontogeny as indicated (y axes).

extent, on the proliferative history of HSCs. This was surprising in light of the evidence demonstrating the quiescent status of adult HSCs during homeostasis and studies showing that HSCs undergo only limited cell divisions over the life span of adult mice (Foudi et al., 2008; Wilson et al., 2008). Strikingly, we found that physiological aged HSCs, as well as HSCs that endured enforced divisional history, were consistently DNA hypermethylated at loci identified as targets of PRC2. Though not conclusive, the reported antagonism between PRC2 and DNA methylation, combined with our data showing diminished expression of the PRC2 core components *Ezh2*, *Suz12*, and *Eed* during aging, suggests that PRC2-mediated repression at these loci may diminish with HSC age and allow the DNA methylation machinery to more readily access these sites.

Evidence that PRC2 may be more broadly involved in regulating the aging, replicative limits, and pathophysiology of diverse cell types is mounting. For example, downregulation of EZH2 leads to BMI1-dependent derepression of the *INK4A-ARF* locus in human and mouse cells undergoing senescence (Agherbi et al., 2009; Bracken et al., 2007), whereas continued ectopic expression of *Ezh2* extends the replicative limits of HSCs (Kamminga et al., 2006). Furthermore, a recent study examining DNA methylation in healthy and cancer patients revealed an age-associated increase in DNA hypermethylation of PRC2 targets (Teschendorff et al., 2010), suggesting that this may be a common feature of aging in diverse cell types. Gains of DNA methylation of PRC2 targets have also been shown to be characteristic of diverse cancers (Deaton and Bird, 2011), whereas loss-of-function mutations in PRC2 core components have been found in a variety of myeloid diseases, including acute myelogenous leukemia and myelodysplastic syndrome (MDS)—the prototypic HSC disease of the elderly (Shih et al., 2012). These facts, together with the fact that mutations in *TET2*, which encodes a DNA demethylase, are among the most common found in MDS patients (Shih et al., 2012), indicate that aberrant DNA hypermethylation in HSCs is likely central to the etiology of disease in these patients. This has been affirmed in clinical trials demonstrating that subsets of MDS patients are responsive to DNA hypomethylating agents (Fukumoto and Greenberg, 2005).

Given the striking functional and molecular conservation of HSC aging in mice and humans (Pang et al., 2011), it will be important to determine if the alterations of the DNA methylation landscape we report here similarly underlie human HSC aging and/or progression to disease. If so, the plasticity and potential reversibility of DNA methylation opens the possibility of therapeutically targeting the DNA methylome or its regulators as a means of restoring function to aged HSCs.

EXPERIMENTAL PROCEDURES

Mice

C57BL/6 males were used as transplant donors and for DNA methylation analysis. Young mice were 12–14 weeks of age. Old mice (22–26 months) were obtained from the National Institute of Aging (Bethesda, MD). All mice were maintained according to Harvard Medical School Animal Facility protocols. Procedures were performed with consent from local ethics committees. 5-FU was administered at 150 mg/kg by intraperitoneal injection.

HSC Purification

Lineage depletion was performed using biotin-conjugated antibodies against CD3, CD4, CD8, B220, Ter119, Mac1, Gr1, and Il7rα and streptavidin-conjugated magnetic beads (Miltenyi). Lineage-depleted cells were stained with antibodies against Sca1, c-kit, CD34, Flk2, CD48, CD150, fluorescently labeled streptavidin, propidium iodide (PI), and, in transplant settings, CD45.1 and CD45.2. HSCs were sorted as $PI^-lin^-c\text{-}kit^+Sca1^+CD34^-Flk2^-CD150^+$ on a FACS Aria II (Becton Dickinson). E14.5 FLs were lineage depleted using biotin-conjugated antibodies to CD3, CD4, CD8, B220, Ter119, Gr1, and Il7rα and streptavidin-conjugated magnetic beads, and then stained with antibodies against Sca1, c-kit, Mac1, CD48, CD150, fluorescently labeled streptavidin, and PI. FL-HSCs were isolated as $PI^-lin^-c\text{-}kit^+Sca1^+CD48^-CD150^+Mac1^+$. PI was used to exclude dead cells. HSCs were double sorted for purity. FACS data were analyzed with FlowJo software (Tree Star, Ashland, OR).

Transplantation Experiments

HSCs were transplanted at indicated cell numbers into lethally irradiated (10 Gy) recipients against 2×10^5 competitor BM cells or 3×10^5 Sca1-depleted BM cells as indicated. Secondary transplants were performed competitively. BM transplant recipients were injected with a total of 2×10^6 cells at a 1:1 ratio of donor to competitor. Peripheral blood analysis was performed at 4 week intervals posttransplant with antibodies against Ter119, B220, Mac1, Gr1, CD3, CD45.1, CD45.2, and PI.

DNA Methylation Analysis

RRBS was performed according to a previously published protocol (Gu et al., 2011; Smith et al., 2009, 2012). The raw sequencing reads were aligned using Maq's bisulfite alignment mode (Li et al., 2008), and DNA methylation calling was performed using custom software (Gu et al., 2010). DNA methylation analysis was performed as previously described (Bock et al., 2012).

Genome-wide Expression Profiling

FACs-purified HSCs from FL (E14.5), young mice (3.5 months), and old mice (25 months) were sorted into TRIzol (Invitrogen). RNA was purified and double amplified (Affymetrix) and hybridized to Affymetrix Mouse 430 2.0 arrays.

Resulting cel files were normalized in R using gcRMA. Comparative analysis was performed using GenePattern (Reich et al., 2006). Normalized files were preprocessed with a fold change of $\leq$2 and a delta of $\leq$50 (linear array values). Comparative marker selection computed p values based on all possible sample permutations. Thresholds for significance were set as the following filters: FDR(BH) $\leq$ 0.05, Feature p $\leq$ 0.001, and Fold Change $\geq$ 2.

Expression data of 39 hematopoietic cell types, GSE34723 (Seita et al., 2012), was renormalized using R. Probe sets used for comparison analysis were determined to be the closest probe set within +10 kb of each differentially methylated region, a placement that also accounted for probe set strand information. A threshold of linear expression value $\geq$50 was used. Pairwise t test comparisons of the expression of each non-HSC cell type to HSCs were performed, and the threshold for significant differences was as follows: fold change $\geq$1.5 and p $\leq$ 0.01. Absolute gene expression images (Figure 2) were generated using "Gene Expression Commons" (Seita et al., 2012).

Quantitative Real-Time PCR

Ten cells were sorted into a modified lysis buffer (Warren et al., 2006), and genes of interest were preamplified using Cells Direct One-step qRT-PCR kit (Invitrogen) with primers spanning intron-exon boundaries designed using PrimerBlast (http://www.ncbi.nlm.nih.gov/tools/primer-blast/). Real-time PCR was performed using nested primers and Kapa SYBR Fast (Kapa Biosystems) with 4 μl of a 10× dilution of preamplified 10 cell samples. γ-actin was used to normalize expression. ΔcT values were generated for each sample and ΔΔcT values are presented.

Telomere Length Assays

Single-cell telomere assays were measured by qPCR as recently described (Norddahl et al., 2012). See also Supplemental Experimental Procedures.

ACCESSION NUMBERS

Raw and processed DNA methylation data (FASTQ and BED files) are available at GEO under accession number GSE44117.

SUPPLEMENTAL INFORMATION

Supplemental Information for this article includes six figures, seven tables, and Supplemental Experimental Procedures and can be found with this article online at http://dx.doi.org/10.1016/j.stem.2013.01.017.

ACKNOWLEDGMENTS

We would like to thank A. Zguro, R. Gazit, L. Fang, and M. Ziller for technical assistance; P. Mandal for helpful discussions; and E. Beerman for editorial help. This work was supported by a grant from the Harvard Stem Cell Institute. A.M. is supported by the Pew Charitable Trusts. D.J.R. and A.M. are New York Stem Cell Foundation, Robertson Investigators.

Received: June 6, 2012
Revised: December 17, 2012
Accepted: January 25, 2013
Published: February 14, 2013

REFERENCES

Adolfsson, J., Månsson, R., Buza-Vidas, N., Hultquist, A., Liuba, K., Jensen, C.T., Bryder, D., Yang, L., Borge, O.J., Thoren, L.A., et al. (2005). Identification of Flt3+ lympho-myeloid stem cells lacking erythro-megakaryocytic potential a revised road map for adult blood lineage commitment. Cell *121*, 295–306.

Agherbi, H., Gaussmann-Wenger, A., Verthuy, C., Chasson, L., Serrano, M., and Djabali, M. (2009). Polycomb mediated epigenetic silencing and replication timing at the INK4a/ARF locus during senescence. PLoS ONE *4*, e5622.

Allsopp, R.C., Cheshier, S., and Weissman, I.L. (2001). Telomere shortening accompanies increased cell cycle activity during serial transplantation of hematopoietic stem cells. J. Exp. Med. *193*, 917–924.

Allsopp, R.C., Morin, G.B., Horner, J.W., DePinho, R., Harley, C.B., and Weissman, I.L. (2003). Effect of TERT over-expression on the long-term transplantation capacity of hematopoietic stem cells. Nat. Med. *9*, 369–371.

Beerman, I., Bhattacharya, D., Zandi, S., Sigvardsson, M., Weissman, I.L., Bryder, D., and Rossi, D.J. (2010a). Functionally distinct hematopoietic stem cells modulate hematopoietic lineage potential during aging by a mechanism of clonal expansion. Proc. Natl. Acad. Sci. USA *107*, 5465–5470.

Beerman, I., Maloney, W.J., Weissmann, I.L., and Rossi, D.J. (2010b). Stem cells and the aging hematopoietic system. Curr. Opin. Immunol. *22*, 500–506.

Benz, C., Copley, M.R., Kent, D.G., Wohrer, S., Cortes, A., Aghaeepour, N., Ma, E., Mader, H., Rowe, K., Day, C., et al. (2012). Hematopoietic stem cell subtypes expand differentially during development and display distinct lymphopoietic programs. Cell Stem Cell *10*, 273–283.

Bock, C., Tomazou, E.M., Brinkman, A.B., Müller, F., Simmer, F., Gu, H., Jäger, N., Gnirke, A., Stunnenberg, H.G., and Meissner, A. (2010). Quantitative comparison of genome-wide DNA methylation mapping technologies. Nat. Biotechnol. *28*, 1106–1114.

Bock, C., Beerman, I., Lien, W.H., Smith, Z.D., Gu, H., Boyle, P., Gnirke, A., Fuchs, E., Rossi, D.J., and Meissner, A. (2012). DNA methylation dynamics during in vivo differentiation of blood and skin stem cells. Mol. Cell *47*, 633–647.

Bracken, A.P., Kleine-Kohlbrecher, D., Dietrich, N., Pasini, D., Gargiulo, G., Beekman, C., Theilgaard-Mönch, K., Minucci, S., Porse, B.T., Marine, J.C., et al. (2007). The Polycomb group proteins bind throughout the INK4A-ARF locus and are disassociated in senescent cells. Genes Dev. *21*, 525–530.

Brinkman, A.B., Gu, H., Bartels, S.J., Zhang, Y., Matarese, F., Simmer, F., Marks, H., Bock, C., Gnirke, A., Meissner, A., and Stunnenberg, H.G. (2012). Sequential ChIP-bisulfite sequencing enables direct genome-scale investigation of chromatin and DNA methylation cross-talk. Genome Res. *22*, 1128–1138.

Bryder, D., Rossi, D.J., and Weissman, I.L. (2006). Hematopoietic stem cells: the paradigmatic tissue-specific stem cell. Am. J. Pathol. *169*, 338–346.

Challen, G.A., Boles, N.C., Chambers, S.M., and Goodell, M.A. (2010). Distinct hematopoietic stem cell subtypes are differentially regulated by TGF-beta1. Cell Stem Cell *6*, 265–278.

Challen, G.A., Sun, D., Jeong, M., Luo, M., Jelinek, J., Berg, J.S., Bock, C., Vasanthakumar, A., Gu, H., Xi, Y., et al. (2012). Dnmt3a is essential for hematopoietic stem cell differentiation. Nat. Genet. *44*, 23–31.

Chambers, S.M., Shaw, C.A., Gatza, C., Fisk, C.J., Donehower, L.A., and Goodell, M.A. (2007). Aging hematopoietic stem cells decline in function and exhibit epigenetic dysregulation. PLoS Biol. *5*, e201.

de Haan, G., Nijhof, W., and Van Zant, G. (1997). Mouse strain-dependent changes in frequency and proliferation of hematopoietic stem cells during aging: correlation between lifespan and cycling activity. Blood *89*, 1543–1550.

Deaton, A.M., and Bird, A. (2011). CpG islands and the regulation of transcription. Genes Dev. *25*, 1010–1022.

Dykstra, B., Kent, D., Bowie, M., McCaffrey, L., Hamilton, M., Lyons, K., Lee, S.J., Brinkman, R., and Eaves, C. (2007). Long-term propagation of distinct hematopoietic differentiation programs in vivo. Cell Stem Cell *1*, 218–229.

Dykstra, B., Olthof, S., Schreuder, J., Ritsema, M., and de Haan, G. (2011). Clonal analysis reveals multiple functional defects of aged murine hematopoietic stem cells. J. Exp. Med. *208*, 2691–2703.

Ewing, K.L., and Tauber, O.E. (1964). Hematological Changes in Aging Male C57bl/6 Jax Mice. J. Gerontol. *19*, 165–167.

Florian, M.C., Dörr, K., Niebel, A., Daria, D., Schrezenmeier, H., Rojewski, M., Filippi, M.D., Hasenberg, A., Gunzer, M., Scharffetter-Kochanek, K., et al. (2012). Cdc42 activity regulates hematopoietic stem cell aging and rejuvenation. Cell Stem Cell *10*, 520–530.

Foudi, A., Hochedlinger, K., Van Buren, D., Schindler, J.W., Jaenisch, R., Carey, V., and Hock, H. (2008). Analysis of histone 2B-GFP retention reveals slowly cycling hematopoietic stem cells. Nat. Biotechnol. *27*, 84–90.

Fukumoto, J.S., and Greenberg, P.L. (2005). Management of patients with higher risk myelodysplastic syndromes. Crit. Rev. Oncol. Hematol. *56*, 179–192.

Gonzalo, S. (2010). Epigenetic alterations in aging. J. Appl. Physiol. *109*, 586–597.

Gu, H., Bock, C., Mikkelsen, T.S., Jäger, N., Smith, Z.D., Tomazou, E., Gnirke, A., Lander, E.S., and Meissner, A. (2010). Genome-scale DNA methylation mapping of clinical samples at single-nucleotide resolution. Nat. Methods *7*, 133–136.

Gu, H., Smith, Z.D., Bock, C., Boyle, P., Gnirke, A., and Meissner, A. (2011). Preparation of reduced representation bisulfite sequencing libraries for genome-scale DNA methylation profiling. Nat. Protoc. *6*, 468–481.

Harrison, D.E., and Astle, C.M. (1982). Loss of stem cell repopulating ability upon transplantation. Effects of donor age, cell number, and transplantation procedure. J. Exp. Med. *156*, 1767–1779.

Hayflick, L., and Moorhead, P.S. (1961). The serial cultivation of human diploid cell strains. Exp. Cell Res. *25*, 585–621.

Kamminga, L.M., Bystrykh, L.V., de Boer, A., Houwer, S., Douma, J., Weersing, E., Dontje, B., and de Haan, G. (2006). The Polycomb group gene Ezh2 prevents hematopoietic stem cell exhaustion. Blood *107*, 2170–2179.

Li, H., Ruan, J., and Durbin, R. (2008). Mapping short DNA sequencing reads and calling variants using mapping quality scores. Genome Res. *18*, 1851–1858.

Mandal, P.K., Blanpain, C., and Rossi, D.J. (2011). DNA damage response in adult stem cells: pathways and consequences. Nat. Rev. Mol. Cell Biol. *12*, 198–202.

Meissner, A., Mikkelsen, T.S., Gu, H., Wernig, M., Hanna, J., Sivachenko, A., Zhang, X., Bernstein, B.E., Nusbaum, C., Jaffe, D.B., et al. (2008). Genome-scale DNA methylation maps of pluripotent and differentiated cells. Nature *454*, 766–770.

Morita, Y., Ema, H., and Nakauchi, H. (2010). Heterogeneity and hierarchy within the most primitive hematopoietic stem cell compartment. J. Exp. Med. *207*, 1173–1182.

Muller-Sieburg, C.E., Cho, R.H., Karlsson, L., Huang, J.F., and Sieburg, H.B. (2004). Myeloid-biased hematopoietic stem cells have extensive self-renewal capacity but generate diminished lymphoid progeny with impaired IL-7 responsiveness. Blood *103*, 4111–4118.

Norddahl, G.L., Wahlestedt, M., Gisler, S., Sigvardsson, M., and Bryder, D. (2012). Reduced repression of cytokine signaling ameliorates age-induced decline in hematopoietic stem cell function. Aging Cell *11*, 1128–1131.

Oh, I.H., and Humphries, R.K. (2012). Concise review: Multidimensional regulation of the hematopoietic stem cell state. Stem Cells *30*, 82–88.

Pang, W.W., Price, E.A., Sahoo, D., Beerman, I., Maloney, W.J., Rossi, D.J., Schrier, S.L., and Weissman, I.L. (2011). Human bone marrow hematopoietic stem cells are increased in frequency and myeloid-biased with age. Proc. Natl. Acad. Sci. USA *108*, 20012–20017.

Pappu, R., Cheng, A.M., Li, B., Gong, Q., Chiu, C., Griffin, N., White, M., Sleckman, B.P., and Chan, A.C. (1999). Requirement for B cell linker protein (BLNK) in B cell development. Science *286*, 1949–1954.

Pawliuk, R., Eaves, C., and Humphries, R.K. (1996). Evidence of both ontogeny and transplant dose-regulated expansion of hematopoietic stem cells in vivo. Blood *88*, 2852–2858.

Rank, G., Sutton, R., Marshall, V., Lundie, R.J., Caddy, J., Romeo, T., Fernandez, K., McCormack, M.P., Cooke, B.M., Foote, S.J., et al. (2009). Novel roles for erythroid Ankyrin-1 revealed through an ENU-induced null mouse mutant. Blood *113*, 3352–3362.

Reich, M., Liefeld, T., Gould, J., Lerner, J., Tamayo, P., and Mesirov, J.P. (2006). GenePattern 2.0. Nat. Genet. *38*, 500–501.

Rossi, D.J., Bryder, D., Zahn, J.M., Ahlenius, H., Sonu, R., Wagers, A.J., and Weissman, I.L. (2005). Cell intrinsic alterations underlie hematopoietic stem cell aging. Proc. Natl. Acad. Sci. USA *102*, 9194–9199.

Rossi, D.J., Bryder, D., Seita, J., Nussenzweig, A., Hoeijmakers, J., and Weissman, I.L. (2007). Deficiencies in DNA damage repair limit the function of haematopoietic stem cells with age. Nature *447*, 725–729.

Rossi, D.J., Jamieson, C.H., and Weissman, I.L. (2008). Stems cells and the pathways to aging and cancer. Cell *132*, 681–696.

Rossi, L., Lin, K.K., Boles, N.C., Yang, L., King, K.Y., Jeong, M., Mayle, A., and Goodell, M.A. (2012). Less is more: unveiling the functional core of hematopoietic stem cells through knockout mice. Cell Stem Cell *11*, 302–317.

Rübe, C.E., Fricke, A., Widmann, T.A., Fürst, T., Madry, H., Pfreundschuh, M., and Rübe, C. (2011). Accumulation of DNA damage in hematopoietic stem and progenitor cells during human aging. PLoS ONE *6*, e17487.

Seita, J., Sahoo, D., Rossi, D.J., Bhattacharya, D., Serwold, T., Inlay, M.A., Ehrlich, L.I., Fathman, J.W., Dill, D.L., and Weissman, I.L. (2012). Gene Expression Commons: an open platform for absolute gene expression profiling. PLoS ONE *7*, e40321.

Shih, A.H., Abdel-Wahab, O., Patel, J.P., and Levine, R.L. (2012). The role of mutations in epigenetic regulators in myeloid malignancies. Nat. Rev. Cancer *12*, 599–612.

Smith, Z.D., Gu, H., Bock, C., Gnirke, A., and Meissner, A. (2009). High-throughput bisulfite sequencing in mammakain genomes. Methods *48*, 226–232.

Smith, Z.D., Chan, M.M., Mikkelsen, T.S., Gu, H., Gnirke, A., Regev, A., and Meissner, A. (2012). A unique regulatory phase of DNA methylation in the early mammalian embryo. Nature *484*, 339–344.

Sudo, K., Ema, H., Morita, Y., and Nakauchi, H. (2000). Age-associated characteristics of murine hematopoietic stem cells. J. Exp. Med. *192*, 1273–1280.

Teschendorff, A.E., Menon, U., Gentry-Maharaj, A., Ramus, S.J., Weisenberger, D.J., Shen, H., Campan, M., Noushmehr, H., Bell, C.G., Maxwell, A.P., et al. (2010). Age-dependent DNA methylation of genes that are suppressed in stem cells is a hallmark of cancer. Genome Res. *20*, 440–446.

Thomas, D.J., Rosenbloom, K.R., Clawson, H., Hinrichs, A.S., Trumbower, H., Raney, B.J., Karolchik, D., Barber, G.P., Harte, R.A., Hillman-Jackson, J., et al.; ENCODE Project Consortium. (2007). The ENCODE Project at UC Santa Cruz. Nucleic Acids Res. *35*(Database issue), D663–D667.

Van Zant, G., and Liang, Y. (2003). The role of stem cells in aging. Exp. Hematol. *31*, 659–672.

Wang, H., Lee, C.H., Qi, C., Tailor, P., Feng, J., Abbasi, S., Atsumi, T., and Morse, H.C., 3rd. (2008). IRF8 regulates B-cell lineage specification, commitment, and differentiation. Blood *112*, 4028–4038.

Wang, J., Sun, Q., Morita, Y., Jiang, H., Gross, A., Lechel, A., Hildner, K., Guachalla, L.M., Gompf, A., Hartmann, D., et al. (2012). A differentiation checkpoint limits hematopoietic stem cell self-renewal in response to DNA damage. Cell *148*, 1001–1014.

Warren, L., Bryder, D., Weissman, I.L., and Quake, S.R. (2006). Transcription factor profiling in individual hematopoietic progenitors by digital RT-PCR. Proc. Natl. Acad. Sci. USA *103*, 17807–17812.

Weinhofer, I., Hehenberger, E., Roszak, P., Hennig, L., and Köhler, C. (2010). H3K27me3 profiling of the endosperm implies exclusion of polycomb group protein targeting by DNA methylation. PLoS Genet. *6*, 6.

Wilson, A., Laurenti, E., Oser, G., van der Wath, R.C., Blanco-Bose, W., Jaworski, M., Offner, S., Dunant, C.F., Eshkind, L., Bockamp, E., et al. (2008). Hematopoietic stem cells reversibly switch from dormancy to self-renewal during homeostasis and repair. Cell *135*, 1118–1129.

Yahata, T., Takanashi, T., Muguruma, Y., Ibrahim, A.A., Matsuzawa, H., Uno, T., Sheng, Y., Onizuka, M., Ito, M., Kato, S., and Ando, K. (2011). Accumulation of oxidative DNA damage restricts the self-renewal capacity of human hematopoietic stem cells. Blood *118*, 2941–2950.